

Electron mass shift in nonthermal systems

P L Hagelstein¹ and I U Chaudhary²

¹ Research Laboratory of Electronics, Massachusetts Institute of Technology, Cambridge, MA 02139, USA

² Department of Computer Science and Engineering, University of Engineering and Technology, Lahore, Pakistan

E-mail: plh@mit.edu, irfanc@mit.edu

Received 24 January 2008, in final form 14 May 2008

Published 6 June 2008

Online at stacks.iop.org/JPhysB/41/125001

Abstract

The electron mass is known to be sensitive to local fluctuations in the electromagnetic field, and undergoes a small shift in a thermal field. It was claimed recently that a very large electron mass shift should be expected near the surface of a metal hydride (Widom and Larsen 2006 *Eur. Phys. J. C* **46** 107). We examine the shift using a formulation based on the Coulomb gauge, which leads to a much smaller shift. The maximization of the electron mass shift under nonequilibrium conditions seems nonetheless to be an interesting problem. We consider a scheme in which a current in a hollow wire produces a large vector potential in the wire centre. Fluctuations in an LC circuit with nearly matched loss and gain can produce large current fluctuations; and these can increase the electron mass shift by orders of magnitude over its room temperature value.

1. Introduction

The problem of the electron self-energy has been of interest since the early days of quantum field theory, most importantly in the case of the vacuum [1] and atoms [2–4]. Subsequently, there has been interest in the electron self-energy under a variety of conditions: in a strong magnetic field [5], in an intense laser radiation field [6, 7] and in a thermal radiation field [8, 9]. Such problems have provided theorists with a rich opportunity for substantive theoretical developments [10]. One of the low-order terms that results from QED is a mass shift. The mass shift due to a thermal field under readily accessible conditions is very small, but an experimental observation has been reported [11]. In the case of an intense laser field, the mass shift can be much greater; however, under these conditions other processes, such as multiphoton ionization, occur [12].

Our interest in this problem generally was stimulated by a recent paper by Widom and Larsen [13]. In this paper, the authors propose that a very large mass shift can be obtained near the surface of a metal hydride under nonequilibrium conditions. According to Widom and Larsen, the electron mass shift can be in the MeV range.

Of course, a mass shift this large is unexpected and unprecedented. To develop such a large mass shift, intuition suggests that the electron must interact with the local environment with at least a comparable interaction strength.

Under the relatively benign environment of a metal hydride, it is difficult to understand why such large interactions should occur. If there existed such strong dynamical fluctuations, one should expect multiphoton ionization as occurs in intense laser field, but generally no such effects are usually observed. Consequently, we are motivated to examine the model in order to better understand the problem.

In their paper, Widom and Larsen obtain mass shift formulae which are Lorentz invariant, or gauge-free. A specific numerical example is given in which the electric field is estimated from a simplified model which is based on the electric field due to oscillating protons at the metal hydride surface. Of interest was whether the Widom and Larsen result could be confirmed in a different formalism in which a specific gauge is specified. Results for observable quantities must be independent of the choice of gauge in the case of a complete computation where all effects are taken into account. It is well known that the choice of gauge can produce different answers in practical computations where the computation is approximate, or not complete in this sense [7, 14]. Since the Coulomb gauge is widely used, we adopted it for this purpose. We find that the mass shift estimated using this approach for their example is lower by the fourth power of the ratio of the proton velocity to the speed of light. In this example, the Coulomb gauge result is lower by about 17 orders of magnitude. Since local electrons have

higher velocities, one would expect a much larger electron–electron contribution, especially if a significant current was present. However, any such effects are trivial in comparison with Coulomb interactions between electrons and ions that occur in a metal hydride.

Nevertheless, an issue underlying the Widom and Larsen paper remains of interest. Can a large mass shift be produced somehow under nonequilibrium conditions, without using an intense laser field, and under conditions where other processes, such as multiphoton ionization, are avoided? To this end, we consider an idealized physical situation (conditions in the centre of a hollow conductor carrying a large current) in which we seek to create a very large vector potential and induce fluctuations that would maximize the mass shift. If the frequency components remain sufficiently low, multiphoton transitions and ionization should be minimized. We find that a small electron mass shift can be generated using this approach, and the effect should be detectable through the observation of line shifts for transitions involving weakly bound electrons.

2. Idealized model

It is often useful to have a highly simplified model in order to gain intuition about an effect. In this case we can take advantage of a similar one that has been used for this purpose previously [15]. Consider an electron in free space interacting with a transverse field according to

$$\hat{H} = \boldsymbol{\alpha} \cdot c\mathbf{p} + \beta mc^2 - \frac{e}{c} \boldsymbol{\alpha} \cdot \hat{\mathbf{A}}. \quad (1)$$

The energy then depends on the transverse radiation field through

$$E^2 = \langle \hat{H}^2 \rangle = (mc^2)^2 + \left\langle \left| c\mathbf{p} - \frac{e}{c} \hat{\mathbf{A}} \right|^2 \right\rangle - \frac{e^2}{c^2} \langle |\hat{\mathbf{A}}|^2 \rangle_0, \quad (2)$$

where we subtract out the vacuum contribution to the fluctuations, since it is already taken into account in the mass m .

2.1. Mass shift in terms of vector potential fluctuations

Assuming an approximate product wavefunction in which the electron and radiation field are taken to be independent, we obtain

$$E^2 = (mc^2)^2 + c^2 \langle |\mathbf{p}|^2 \rangle - e \langle \mathbf{p} \rangle \cdot \langle \hat{\mathbf{A}} \rangle - e \langle \hat{\mathbf{A}} \rangle \cdot \langle \mathbf{p} \rangle + \frac{e^2}{c^2} [\langle |\hat{\mathbf{A}}|^2 \rangle - \langle |\hat{\mathbf{A}}|^2 \rangle_0]. \quad (3)$$

We introduce a shifted momentum

$$\langle \mathbf{p}' \rangle = \langle \mathbf{p} \rangle - \frac{e}{c} \langle \hat{\mathbf{A}} \rangle \quad (4)$$

to obtain

$$E^2 = (mc^2)^2 + c^2 \langle |\mathbf{p}'|^2 \rangle + \frac{e^2}{c^2} (\langle |\hat{\mathbf{A}}|^2 \rangle - \langle |\hat{\mathbf{A}}|^2 \rangle_0 - \langle \hat{\mathbf{A}} \rangle^2). \quad (5)$$

From this we can identify the dressed mass in terms of electromagnetic field fluctuations according to

$$(m^*)^2 = m^2 + \frac{e^2}{c^4} (\langle |\hat{\mathbf{A}}|^2 \rangle - \langle |\hat{\mathbf{A}}|^2 \rangle_0 - \langle \hat{\mathbf{A}} \rangle^2). \quad (6)$$

The mass shift δm is then

$$\delta m = \frac{e^2}{2mc^4} (\langle |\hat{\mathbf{A}}|^2 \rangle - \langle |\hat{\mathbf{A}}|^2 \rangle_0 - \langle \hat{\mathbf{A}} \rangle^2) \quad (7)$$

under the assumption that $\delta m \ll m$.

If a Coulomb potential is present, then the above simplified argument can be replaced with a rotation of the Dirac Hamiltonian using a Foldy–Wouthuysen transformation [16, 17], followed by taking appropriate expectation values. The Foldy–Wouthuysen transformation has also been used to rotate field operators [18], which provides an alternate starting place for the development of the mass shift formula.

2.2. Mass shift in a thermal radiation field

In the event that the local radiation field is a blackbody, the expectation value of the potential vector $\langle \hat{\mathbf{A}} \rangle$ is zero, and one obtains [8, 9]

$$\frac{\delta m}{m} = \frac{\pi\alpha}{3} \left[\frac{k_B T}{mc^2} \right]^2. \quad (8)$$

2.3. Need for a quantum kinetic formulation

The argument presented here is useful in that it motivates simply why one might make a connection between vector potential fluctuations and the electron mass shift. However, it is not intended to imply that this is the whole story.

As argued by one of the referees, to compute a shift in the electron mass correctly one must first have an appropriate definition of the electron mass consistent with QED. This suggests that a more appropriate starting place for such a computation would be in the context of a quantum kinetic formulation. Such a calculation would focus on the electron propagator, and include the effects of electromagnetic field interactions from relevant nearby sources. Only in the context of such a formulation would it be possible to obtain a rigorous result for the electron mass shift. Such a program has been carried out in the case of a thermal radiation field [10], with the result that thermal mass shift in the low-temperature regime is in agreement with equation (7) evaluated using thermal fluctuations. However, no similar formulation has yet been reported for the more general case of nonthermal fields, such as are of interest in this work. Consequently, the use of the term electron mass shift in association with fluctuations in the vector potential is not on solid foundation, and a more rigorous treatment is required to establish such a foundation.

3. Mass shift in terms of current sources

If the system is not in thermal equilibrium, we require an expression for the field fluctuations in terms of sources responsible for the local fields. For this, we are guided by the classical problem. The classical vector potential in the Coulomb gauge satisfies

$$-\nabla \times \left[\frac{1}{\mu} \nabla \times \mathbf{A}(\mathbf{r}, \omega) \right] + \frac{\omega^2 \epsilon}{c^2} \mathbf{A}(\mathbf{r}, \omega) = -\frac{4\pi}{c} \mathbf{j}(\mathbf{r}, \omega) \quad (9)$$

subject to

$$\nabla \cdot \mathbf{A}(\mathbf{r}, \omega) = 0 \quad (10)$$

which defines the Coulomb gauge. This subsidiary condition can be omitted if we replace the current density by \mathbf{j}_T , where \mathbf{j}_T is the transverse part of the current density [19]. The classical vector potential arising from sources can be constructed from those sources according to

$$\mathbf{A}(\mathbf{r}, \omega) = \frac{1}{c} \int d^3\mathbf{r}' G(\mathbf{r}, \mathbf{r}'; \omega) \mathbf{j}_T(\mathbf{r}', \omega), \quad (11)$$

where the Green's function $G(\mathbf{r}, \mathbf{r}', \omega)$ satisfies

$$\begin{aligned} -\nabla \times \left[\frac{1}{\mu} \nabla \times G_{ij}(\mathbf{r}, \mathbf{r}'; \omega) \right] + \frac{\omega^2 \epsilon}{c^2} G_{ij}(\mathbf{r}, \mathbf{r}'; \omega) \\ = -4\pi \delta_j \delta^3(\mathbf{r} - \mathbf{r}'). \end{aligned} \quad (12)$$

For simplicity we assume spatial uniformity, in which case the Green's function is a scalar. The analogous Heisenberg operators satisfy similar relations, which allows us to write

$$\hat{\mathbf{A}}(\mathbf{r}, \omega) = \frac{1}{c} \int d^3\mathbf{r}' G(\mathbf{r}, \mathbf{r}'; \omega) \hat{\mathbf{j}}_T(\mathbf{r}', \omega). \quad (13)$$

We can then relate the electromagnetic field fluctuations to fluctuations in the source according to

$$\begin{aligned} \langle \hat{\mathbf{A}}(\mathbf{r}, \omega) \cdot \hat{\mathbf{A}}(\mathbf{r}, \omega) \rangle - \langle \hat{\mathbf{A}}(\mathbf{r}, \omega) \rangle \cdot \langle \hat{\mathbf{A}}(\mathbf{r}, \omega) \rangle \\ = \frac{1}{c^2} \int d^3\mathbf{r}' \int d^3\mathbf{r}'' G(\mathbf{r}, \mathbf{r}'; \omega) G(\mathbf{r}, \mathbf{r}''; \omega) \\ \times [\langle \hat{\mathbf{j}}_T(\mathbf{r}', \omega) \cdot \hat{\mathbf{j}}_T(\mathbf{r}'', \omega) \rangle - \langle \hat{\mathbf{j}}_T(\mathbf{r}', \omega) \rangle \cdot \langle \hat{\mathbf{j}}_T(\mathbf{r}'', \omega) \rangle]. \end{aligned} \quad (14)$$

A related approach was used in [20] for electromagnetic field fluctuations near surfaces. Hence, we may write for the relative mass shift

$$\begin{aligned} \frac{\delta m}{m} = \int d\omega \frac{1}{2} \left(\frac{e}{mc^3} \right)^2 \int d^3\mathbf{r}' \int d^3\mathbf{r}'' G(\mathbf{r}, \mathbf{r}'; \omega) G(\mathbf{r}, \mathbf{r}''; \omega) \\ \times [\langle \hat{\mathbf{j}}_T(\mathbf{r}', \omega) \cdot \hat{\mathbf{j}}_T(\mathbf{r}'', \omega) \rangle - \langle \hat{\mathbf{j}}_T(\mathbf{r}', \omega) \rangle \cdot \langle \hat{\mathbf{j}}_T(\mathbf{r}'', \omega) \rangle]. \end{aligned} \quad (15)$$

4. Mass shift in a metal hydride

As discussed in the introduction, Widom and Larsen have identified metal hydrides as an environment in which the mass shift can become large [13]. Electromagnetic field fluctuations in the vicinity of a metal surface have been studied previously [21], and significant near-surface enhancements are reported [22]. However, the mass shift estimate reported in [13] seems to be larger than what we would expect, so in this section we examine the model used.

4.1. Widom–Larsen model

To obtain an estimate for the mass shift, these authors have expressed the dressed mass (translated into our notation) as

$$\frac{m^*}{m} = \sqrt{1 + \left(\frac{e}{mc^2} \right)^2 A^\mu A_\mu} \quad (16)$$

which is developed into

$$\frac{m^*}{m} = \sqrt{1 + \frac{|\bar{\mathbf{E}}|^2}{\mathcal{E}^2}} \quad (17)$$

with

$$\mathcal{E} = \left| \frac{mc\tilde{\Omega}}{e} \right| \quad (18)$$

with $\tilde{\Omega}$ the local plasma frequency. According to Widom and Larsen, their equation (16) (equation (17) here) is ‘an obviously gauge invariant result’.

To develop a quantitative estimate for the magnitude of the electric field fluctuations, Widom and Larsen consider oscillations of a proton in a local pocket of electronic charge density $-|e|\tilde{n}$. Using Gauss's law, they obtain an estimate for the electric field fluctuations

$$\sqrt{|\bar{\mathbf{E}}|^2} \approx \frac{4e\sqrt{|\mathbf{u}|^2}}{3a_0^3} \quad (19)$$

where \mathbf{u} is the displacement of the proton monolayer and a_0 is the Bohr radius. The estimates that result from this approach lead to estimates for the dressed mass that can be enormous. According to their equation (20), they find

$$\frac{m^*}{m} \approx 20.6. \quad (20)$$

Such a large estimate for the mass shift provided us with the motivation to examine the model.

4.2. Electric field operators

To make progress, we would like to think about the mass shift in terms of the electric field operator. We begin by considering the classical electric field, which can be separated into longitudinal and transverse pieces

$$\mathbf{E} = \mathbf{E}_L + \mathbf{E}_T \quad (21)$$

which satisfy

$$\nabla \times \mathbf{E}_L = 0, \quad \nabla \cdot \mathbf{E}_T = 0. \quad (22)$$

The transverse part is related to the vector potential through

$$\mathbf{E}_T = -\frac{1}{c} \frac{\partial \mathbf{A}}{\partial t}. \quad (23)$$

The analogous Heisenberg operators satisfy the same relation, so we may write

$$\hat{\mathbf{E}}_T(\mathbf{r}, t) = -\frac{1}{c} \frac{\partial \hat{\mathbf{A}}(\mathbf{r}, t)}{\partial t}. \quad (24)$$

We can recast the mass shift formula in terms of the transverse electric field operator by using the Fourier transform version of this relation:

$$\delta m = \frac{e^2}{2mc^2} \int \frac{d\omega}{\omega^2} [\langle |\hat{\mathbf{E}}_T(\omega)|^2 \rangle - \langle |\hat{\mathbf{E}}_T(\omega)|^2 \rangle_0 - |\langle \hat{\mathbf{E}}_T(\omega) \rangle|^2]. \quad (25)$$

In the formulation of Widom and Larsen [13], the appearance of the full electric field operator in their mass shift formula is what makes their gauge invariant formulation different from the Coulomb gauge approach under discussion here. Since the vector potential is related to the transverse electric field operator, only the transverse electric field fluctuations would contribute to the mass shift.

4.3. Ratio of transverse to longitudinal electric field

Of interest in this discussion is an estimate of how large a mass shift should one expect if fluctuations in the transverse electric field were used instead of fluctuations in the longitudinal electric field. To address this, we assume for simplicity that the fluctuations scale with field strength (a nontrivial assumption since fluctuations in the longitudinal field are due to fluctuations in position, which fluctuations in the transverse field are due to fluctuations in momentum). If we know the ratio of the transverse to longitudinal fields near a moving charge, then we can scale the fluctuations accordingly to develop a correction to the mass shift estimate.

For the purposes of developing a simple scaling argument, the Coulomb field in the vicinity of a point charge has a magnitude of

$$|\mathbf{E}_L| \sim \frac{e}{d^2} \quad (26)$$

where d is the distance from the charge. The magnitude of the vector potential in the vicinity of an oscillating charge is

$$|\mathbf{A}| \sim \frac{ev}{cd} \quad (27)$$

where v is the velocity of the charge. The transverse electric field at a frequency ω is then

$$|\mathbf{E}_T| \sim \frac{\omega ev}{c^2 d}. \quad (28)$$

The ratio of the transverse field to longitudinal field is then

$$\frac{|\mathbf{E}_T|}{|\mathbf{E}_L|} \sim \frac{v\omega d}{c^2}. \quad (29)$$

If the range of the moving charge is on the order of the distance with the observer

$$d \sim \frac{v}{\omega} \quad (30)$$

then

$$\frac{|\mathbf{E}_T|}{|\mathbf{E}_L|} \sim \left(\frac{v}{c}\right)^2. \quad (31)$$

The ratio of the mass shift estimate using the transverse electric field to that using the longitudinal electric field, if no other feature of the model is changed, becomes

$$\left[\frac{\delta m}{m}\right]_{\text{CG}} \sim \left[\frac{\delta m}{m}\right]_{\text{WL}} \left(\frac{v}{c}\right)^4 \quad (32)$$

where the subscript CG is for Coulomb gauge, and where the subscript WL is for Widom and Larsen.

4.4. Oscillation frequency and scaled mass shift

If we assume as discussed above that the relative level of fluctuations is the same for longitudinal and transverse fields, then we need an estimate of the proton velocity to complete the estimate. If we adopt a high value for the oscillation frequency from neutron scattering measurements in NbH [23], where $\hbar\omega \sim 100$ meV, and a large estimate for the proton range of 1 \AA , the resulting ratio of the proton velocity to the speed of light is on the order of

$$\frac{v}{c} \sim 5 \times 10^{-5}. \quad (33)$$

In this case, the mass shift obtained using the Coulomb gauge would be on the order of

$$\left[\frac{\delta m}{m}\right]_{\text{CG}} \sim 6 \times 10^{-18} \left[\frac{\delta m}{m}\right]_{\text{WL}}. \quad (34)$$

A mass ratio of 20 estimated using a longitudinal field then would correspond to a shift in energy of less than 10^{-10} eV in a Coulomb gauge calculation.

4.5. Summary and issues

The notion that an electron bound to a proton in a metal hydride could acquire a mass shift on the order of an MeV due to the motion of the proton as part of collective oscillations seems highly unlikely. A simple way to view the effect in the Coulomb gauge can be summed up as follows. The proton oscillates, creating a weak local magnetic field. Fluctuations in the proton velocity then result in fluctuations in the associated magnetic field. These fluctuations give rise to a small mass shift through equation (7).

Since the local electrons can move much faster, the transverse fields developed by surface plasmon oscillations have the potential to give rise to a larger mass shift. Even so, such effects are tiny compared to conventional (Coulombic) orbital interactions that electrons experience in a metal or metal hydride.

5. Mass shift inside a hollow current-carrying wire

Since fluctuations in the vector potential can contribute to an electron mass shift, we are motivated to seek ways to increase the effect. In the measurements of Hollberg and Hall [11], the thermal shift between a weakly bound electron (which experiences the full shift) and a more tightly bound electron (which is shifted very little [24]) was detected as a fractional shift on the order of 2×10^{-12} at 300 K. At higher temperature, the mass shift is larger by the square of the temperature, so an increase of two orders of magnitude seems possible through heating. However, perhaps even larger effects can be obtained through the use of nonequilibrium conditions.

Here, we consider a configuration in which a large current is carried in a hollow wire, in which a large vector potential is produced at the centre. Fluctuations in the vector potential in such a device should produce a mass shift in free (or nearly free) electrons. This can be diagnosed spectroscopically if a gas sample is placed inside the wire. We are interested then in maximizing fluctuations in the vector potential in order to maximize the effect.

5.1. Hollow wire configuration

For this purpose, consider the hollow wire configuration illustrated in figure 1. The inner conductor (made up of a number of windings) carries a strong (and noisy) current which generates a magnetic field \mathbf{H} within, and outside, the conductor. Surrounding this inner conductor is a magnetic material which serves to create a large (and noisy) magnetic flux density \mathbf{B} . The outer conductor carries the return current, and helps confine the magnetic field. An experimental cell

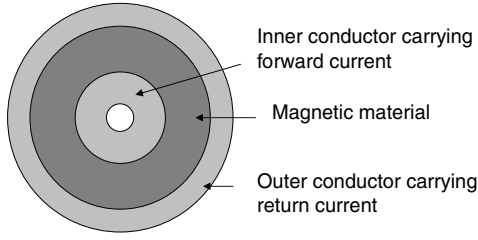


Figure 1. Hollow wire configuration. The inner conductor (light grey) carries the forward current; the outer conductor (light grey) carries the return current; the magnetic material in between (dark grey) maximizes the magnetic flux density.

can be placed inside the inner conductor for spectroscopic tests. The vector potential inside the cell comes about as a result of the surrounding magnetic flux density. Fluctuations in the current result in fluctuations in the magnetic field, causing fluctuations in the magnetic flux density, producing fluctuations in the vector potential, leading ultimately to a mass shift.

5.2. The vector potential

The magnetic field distribution in the quasi-static limit is given in appendix A. From the resulting magnetic flux density, the vector potential along the axis in the centre of the hollow wire configuration is calculated. In the event that the magnetic flux density from the magnetic element of the configuration dominates, the on-axis vector potential is

$$A_z(0) = \frac{2N\mu I}{c} \ln \frac{R_2}{R_1}, \quad (35)$$

where N is the number of windings, μ is the permeability of the magnetic element, I is the current, and R_2/R_1 is the ratio of outer to inner radius of the magnetic material.

This approach is conceptually simple, and is capable of generating large vector potentials. Consider an example in which the classical current I is taken to be 1 A (which is 2.998×10^9 statamps since our formulae are in cgs), and the number of windings N is taken to be unity. The on-axis classical vector potential produced will be 0.1 statvolts (29.98 V) times μ (assuming the logarithmic term is unity for this exercise). In the case of transformer iron ($\mu = 4000$), the resulting vector potential is 400 statvolts (120 kV). For μ -metal ($\mu = 20\,000$), we obtain 2000 statvolts (600 kV). We conclude that quite high vector potentials can be generated using this approach with only modest experimental requirements.

5.3. Mass shift in terms of current fluctuations

However, the mass shift is sensitive to quantum fluctuations in the vector potential, and not to the expectation value (which corresponds to the classical estimate above). Sizeable fluctuations are difficult to generate, as we see in the following section. In this case, we may write

$$\delta m = \frac{2N^2 e^2 \mu^2}{mc^6} \left(\ln \frac{R_2}{R_1} \right)^2 [\langle \hat{I}^2 \rangle - \langle \hat{I} \rangle^2] \quad (36)$$

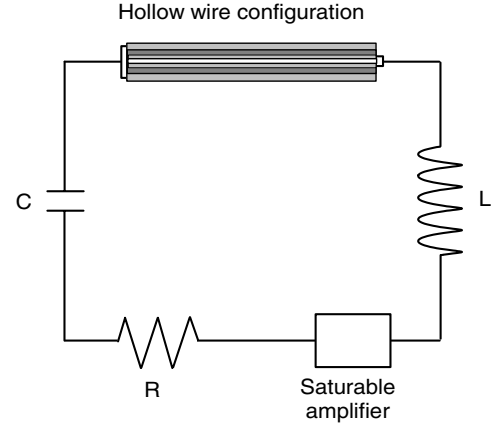


Figure 2. Circuit to supply oscillating current with large fluctuations to the hollow cylinder configuration.

which assumes a mass shift much smaller than the vacuum mass ($\delta m \ll m$).

6. Quantum fluctuations in a lossy driven circuit

So, under what conditions can these fluctuations be maximized? The literature contains numerous papers concerned with the minimization of noise, but in this case we would like to maximize the quantum noise. One approach to the problem is to use a lossy LC-circuit with an amplifier as indicated in figure 2. This circuit is intended to implement the components that occur in a single-mode laser (an oscillator, loss and gain that saturates), which is known to be very noisy when driven near threshold.

6.1. Master equation

To model intensity fluctuations in the single-mode laser (and hence in this kind of circuit), a master equation for the photon probability distribution $p(n, t)$ has been used [25]:

$$\begin{aligned} \frac{\partial}{\partial t} p(n, t) = & \alpha [np(n-1, t) - (n+1)p(n, t)] \\ & - \beta [n^2 p(n-1, t) - (n+1)^2 p(n, t)] \\ & + \gamma [(n+1)p(n+1, t) - np(n, t)]. \end{aligned} \quad (37)$$

The first term on the RHS accounts for linear gain, where α is a gain parameter. Gain saturation to lowest order is modelled by the second term on the RHS, where β is a saturation parameter. The third term accounts for loss, where γ is the loss parameter.

In the steady state, the probability distribution satisfies

$$p(n) = \frac{\alpha/\gamma}{1 + (\beta/\alpha)n} p(n-1) \quad (38)$$

from which an exact solution can be constructed:

$$p(n) \sim \frac{(\alpha^2/\beta\gamma)^n}{\Gamma[(\alpha/\beta) + n + 1]}. \quad (39)$$

6.2. Fluctuations in photon number above threshold

In [25] it is shown that the Stirling approximate can be used to approximate this by a Gaussian, which can be written as

$$p(n) \sim e^{-\frac{1}{2}(n-\langle n \rangle)^2/\Delta n^2} \quad (40)$$

as long as the average number of quanta $\langle n \rangle$ is much greater than the spread Δn . The average $\langle n \rangle$ and spread Δn in this model are given by

$$\langle n \rangle = \frac{\alpha - \gamma}{\beta} \quad \Delta n = \sqrt{\frac{\alpha}{\beta}}. \quad (41)$$

Steady-state fluctuations in this model are maximized when the gain is very nearly matched by the loss ($\alpha \approx \gamma$) for an amplifier with a very low saturation parameter β . We can define a difference parameter δ that is the normalized difference between the gain and loss

$$\delta = \frac{\alpha - \gamma}{\alpha}. \quad (42)$$

In terms of this parameter, the relative fluctuations are

$$\frac{\Delta n}{\langle n \rangle} = \frac{1}{\sqrt{\langle n \rangle} \delta}. \quad (43)$$

The spread Δn for a classical state is simply $\sqrt{\langle n \rangle}$. The fluctuations here are larger by a factor of $1/\sqrt{\delta}$ due to the diffusion in n associated with the loss and gain in the master equation.

6.3. Current fluctuations above threshold

Fluctuations in the current can be determined from fluctuations in number and phase through a perturbative approach. The expectation value of the current can be related to expectation values of number \hat{n} and phase $\hat{\phi}$ according to

$$\langle \hat{I} \rangle = \sqrt{\frac{\hbar \omega_0 \langle \hat{n} \rangle}{2L}} \cos(\omega_0 t + \langle \hat{\phi} \rangle). \quad (44)$$

We use L for the total inductance of the circuit, and where the characteristic frequency of the circuit ω_0 satisfies

$$\omega_0^2 = \frac{1}{LC} \quad (45)$$

where C is the capacitance. If the fluctuations are small relative to the average (as depicted in figure 3), then we can linearize around the sinusoid to obtain

$$\begin{aligned} \hat{I} - \langle \hat{I} \rangle &= \frac{1}{2} \sqrt{\frac{\hbar \omega_0 \langle \hat{n} \rangle}{2L}} \cos(\omega_0 t + \langle \hat{\phi} \rangle) \left(\frac{\hat{n} - \langle \hat{n} \rangle}{\langle \hat{n} \rangle} \right) \\ &\quad - \sqrt{\frac{\hbar \omega_0 \langle \hat{n} \rangle}{2L}} \sin(\omega_0 t + \langle \hat{\phi} \rangle) (\hat{\phi} - \langle \hat{\phi} \rangle). \end{aligned} \quad (46)$$

The fluctuations in the current are then given by

$$\begin{aligned} \langle (\hat{I} - \langle \hat{I} \rangle)^2 \rangle &= \frac{1}{4} \left(\frac{\hbar \omega_0 \langle \hat{n} \rangle}{2L} \right) \cos^2(\omega_0 t + \langle \hat{\phi} \rangle) \left[\frac{\langle (\hat{n} - \langle \hat{n} \rangle)^2 \rangle}{\langle \hat{n} \rangle^2} \right] \\ &\quad - \left(\frac{\hbar \omega_0 \langle \hat{n} \rangle}{2L} \right) \cos(\omega_0 t + \langle \hat{\phi} \rangle) \sin(\omega_0 t + \langle \hat{\phi} \rangle) \\ &\quad \times \left[\frac{(\hat{n} - \langle \hat{n} \rangle)(\hat{\phi} - \langle \hat{\phi} \rangle)}{\langle \hat{n} \rangle} \right] \\ &\quad + \left(\frac{\hbar \omega_0 \langle \hat{n} \rangle}{2L} \right) \sin^2(\omega_0 t + \langle \hat{\phi} \rangle) \langle (\hat{\phi} - \langle \hat{\phi} \rangle)^2 \rangle. \end{aligned} \quad (47)$$

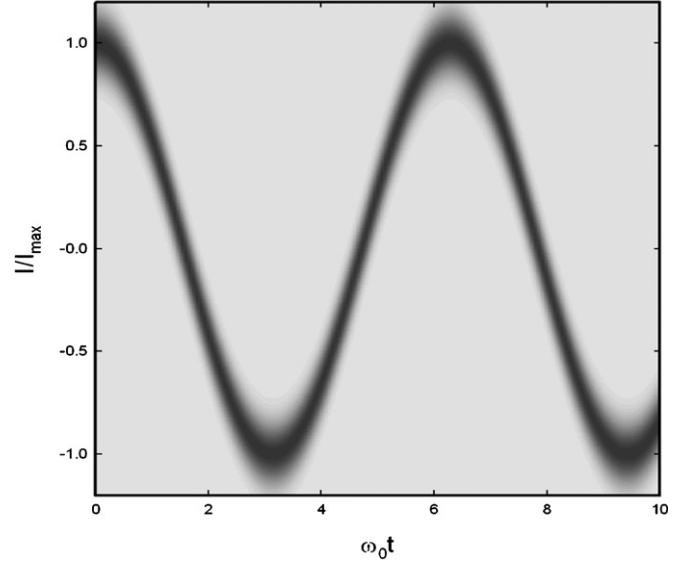


Figure 3. Sinusoidal signal with fluctuations.

The current fluctuations are due to number fluctuations alone when

$$\sin(\omega_0 t + \langle \hat{\phi} \rangle) = 0.$$

In this case we obtain

$$\langle (\hat{I} - \langle \hat{I} \rangle)^2 \rangle = \frac{1}{4} \langle \hat{I} \rangle_{\max}^2 \left[\frac{\langle (\hat{n} - \langle \hat{n} \rangle)^2 \rangle}{\langle \hat{n} \rangle^2} \right]. \quad (48)$$

6.4. Current fluctuations below threshold

When run below threshold, the excitation of the oscillator is much weaker, so that we can neglect saturation. In this case we obtain a thermal distribution in the steady state

$$p(n) = \frac{\alpha}{\gamma} p(n-1) = e^{-\hbar \omega_0 / k_B T_{\text{eff}}} p(n-1), \quad (49)$$

where T_{eff} is the effective temperature associated with the amplifier and loss. In the high-temperature limit, the current fluctuations are

$$\langle \hat{I}^2 \rangle - \langle \hat{I} \rangle^2 = \frac{\hbar \omega_0}{L} \left[\frac{1}{e^{\hbar \omega_0 / k_B T_{\text{eff}}} - 1} + \frac{1}{2} \right] \rightarrow \frac{k_B T_{\text{eff}}}{L}. \quad (50)$$

6.5. Mass shift estimates

We can use these results to develop estimates for the mass shift. Above threshold, the current fluctuations appear in connection with an oscillating signal, and are limited by how closely the gain matches the loss. Below threshold, only fluctuations occur, and the effective noise temperature is determined once again by how closely the gain matches the loss. In the circuit that we examined here, the gain and loss are variable, but in the steady-state solutions we assumed that they remain fixed. In practice, one would use a more sophisticated arrangement with a very hot resistive element to inject noise (not included in our master equation) and feedback to keep the gain and loss closely matched (not included in our model). Consequently,

it makes sense here to characterize the noise in terms of an effective temperature in order to evaluate the magnitude of the mass shift and associated energy shift.

From this discussion, we may write the mass shift in terms of the effective temperature for the below-threshold case as

$$\delta m = \frac{2N^2 e^2 \mu^2 k_B T_{\text{eff}}}{mc^6 L} \left(\ln \frac{R_2}{R_1} \right)^2 \quad (\text{below threshold}). \quad (51)$$

Before continuing, we note that the mass shift is maximized when the inductance is minimized, so that no additional inductance should be used. In this case, the total inductance for the circuit is very nearly that of the hollow wire (L_{hw}), which is given in the appendix to be

$$L_{hw} = \frac{2N^2 \mu l_z}{c^2} \ln \frac{R_2}{R_1}, \quad (52)$$

where l_z is the length of the hollow wire. Upon inserting, we obtain for the mass shift

$$\delta m = \frac{e^2 \mu k_B T_{\text{eff}}}{mc^4 l_z} \ln \frac{R_2}{R_1} \quad (\text{below threshold}). \quad (53)$$

The associated energy shift evaluates to

$$\delta mc^2 = 5.63 \times 10^{-10} \text{ eV} \ln \frac{R_2}{R_1} \left[\frac{10 \text{ cm}}{l_z} \right] \left[\frac{\mu}{20000} \right] \left[\frac{k_B T_{\text{eff}}}{1 \text{ eV}} \right]. \quad (54)$$

Based on this, we would expect that energy shifts in the range of 10^{-9} – 10^{-6} eV should be possible by maximizing the noise temperature, and by taking advantage of more advanced magnetic materials.

7. Summary and conclusions

Our effort was stimulated by the recent publication of Widom and Larsen who proposed that a large electron mass shift could be expected to occur near the surface of a metal hydride [13]. These authors were led to this conclusion from a gauge-free formulation of the mass shift. Since the result is so counter to our intuition, we decided to investigate an approach based on the Coulomb gauge. In the end, the key difference is that in the Coulomb gauge one must use the transverse electric field fluctuations for a mass shift estimate instead of fluctuations in the longitudinal field. As a result, the mass shift that we would expect would be orders of magnitude smaller.

As a result of the Widom and Larsen proposal, we were motivated to consider the problem of creating a more significant mass shift than can be obtained thermally, by using nonequilibrium conditions to maximize the fluctuations in the potential vector. To this end, we proposed the use of a hollow wire with a magnetic element driven by a noisy current source; the mass shift in such a configuration is proportional to the current fluctuations of the circuit. To maximize current fluctuations, we considered a lossy LC circuit with an amplifier, which is closely related to the problem of a single-mode laser which is known to be extremely noisy near threshold. Fluctuations in the oscillator photon number were modelled using a simple master equation borrowed from laser physics, which has been used to describe the photon

distribution in a single-mode laser. Above threshold the signal is oscillatory with small fluctuations which are maximized near threshold. Below threshold, the photon distribution is thermal at a temperature determined by the ratio of the gain to the loss; near threshold, the gain very nearly matches the loss, and the effective temperature can be very high.

To maximize the mass shift, the circuit inductance should be minimized. When the inductance of the hollow wire dominates the circuit inductance, the below-threshold mass shift depends on the permeability, the geometry of the cylinder and on the noise temperature. It is independent of the number of windings. The mass shift induced in this way is sufficiently large to be observable (we believe that energy shifts in the range of 10^{-9} – 10^{-6} eV can be produced in a free, or weakly-bound, electron), and it can be greater than the thermal shift observed previously near room temperature. The development of very high noise temperatures in the circuit (in the keV range or higher) will require the use of a more sophisticated circuit than that analysed here, since it is difficult to match the gain and loss so precisely without feedback.

Note that the mass shift produced in such an experiment occurs under conditions where the classical electric and magnetic fields are zero (in the above threshold case, we are focused on the $\sin(\omega t + \langle \hat{\phi} \rangle) = 0$ condition in which the expectation value of the transverse electric field is zero). It appears as if the electron is exhibiting a response to the vector potential in such an experiment.

Acknowledgments

The authors take pleasure in acknowledging support for this work from a gift from David Griswold, and a gift from the New York Trust.

Appendix. Classical vector potential estimate

In this appendix we consider the vector potential due to a simple hollow wire configuration as illustrated in figure 1. The innermost hollow cylinder (between R_0 and R_1) is a conductor for the forward current, assumed to be made from a nonmagnetic metal such as copper. This conductor is surrounded by a magnetic material (between R_1 and R_2) such as iron or permalloy. An outer cylindrical conductor is present to carry a return current.

A.1. Magnetic field

If we assume that the current is carried uniformly in the nonmagnetic conductors, and that the system is magneto-quasistatic, then we can estimate the magnetic field using

$$\oint_C \mathbf{H} \cdot d\mathbf{l} = \frac{4\pi}{c} \int \mathbf{J} \cdot \hat{\mathbf{n}} d^2a \quad (A.1)$$

using circular contours at different radial distances ρ away from the centre. We assume that the current in the inner hollow cylinder is z -directed

$$\mathbf{J} = \hat{\mathbf{z}} J_0 \quad (\text{inner conductor}). \quad (A.2)$$

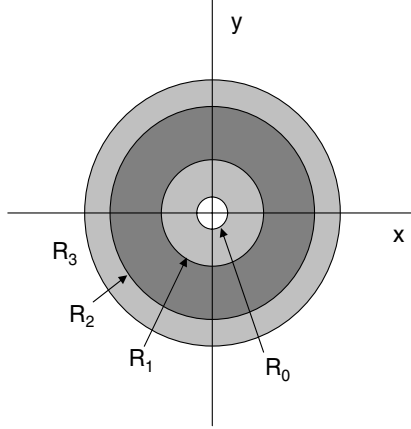


Figure 1. Cross section of a simple hollow wire configuration. The centre is hollow, out to a radius R_0 (indicated in white). An inner conductor is shown between R_0 and R_1 (in light grey). A magnetic material with permeability μ is indicated between R_1 and R_2 (in dark grey). An outer nonmagnetic conductor to carry the return current is illustrated between R_2 and R_3 (in light grey).

The outer cylinder carries the return current, and is also z -directed

$$\mathbf{J} = -\hat{\mathbf{i}}_z J_1 \quad (\text{outer conductor}). \quad (\text{A.3})$$

The magnetic field is ϕ -directed, and can be estimated simply from equation (A.1),

$$\mathbf{H}(\rho) = \begin{cases} 0 & 0 \leq \rho \leq R_0 \\ \hat{\mathbf{i}}_\phi \frac{2\pi J_0}{\rho c} (\rho^2 - R_0^2) & R_0 \leq \rho \leq R_1 \\ \hat{\mathbf{i}}_\phi \frac{2\pi J_0}{\rho c} (R_1^2 - R_0^2) & R_1 \leq \rho \leq R_2 \\ \hat{\mathbf{i}}_\phi \left[\frac{2\pi J_0}{\rho c} (R_1^2 - R_0^2) - \frac{2\pi J_1}{\rho c} (\rho^2 - R_2^2) \right] & R_2 \leq \rho \leq R_3 \\ 0 & \rho > R_3. \end{cases} \quad (\text{A.4})$$

The magnetic field is zero outside since the return current matches the forward current

$$J_0\pi(R_1^2 - R_0^2) = J_1\pi(R_3^2 - R_2^2). \quad (\text{A.5})$$

A.2. Vector potential

The vector potential at the z -axis can be found from

$$\oint_C \mathbf{A} \cdot d\mathbf{l} = \int \mu \mathbf{H} \cdot d^2a. \quad (\text{A.6})$$

For this we use a rectangular contour that travels a short distance Δz along the z -axis; then radially outward beyond the outer conductor; then backward the same distance in z ; and then radially inward. Since the magnetic field is ϕ -directed, no contribution is obtained for the radial legs. Hence, we obtain

$$\begin{aligned} [A_z(0) - A_z(R_3)]\Delta z \\ = \Delta z \int_{R_0}^{R_1} \frac{2\pi J_0}{\rho c} (\rho^2 - R_0^2) d\rho \end{aligned}$$

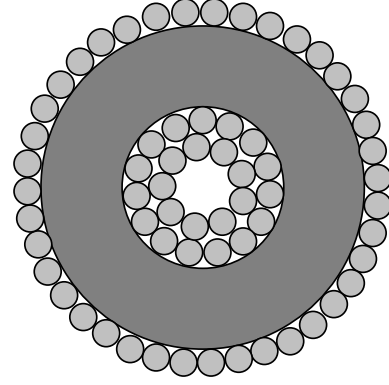


Figure 2. Cross section of a looped configuration. A wire (light grey) is looped around a cylindrical shell of magnetic material (dark grey) N times. A single wire carries the current I , but the total current passing inside the magnetic material is NI .

$$\begin{aligned} + \Delta z \int_{R_1}^{R_2} \frac{2\pi \mu J_0}{\rho c} (R_1^2 - R_0^2) d\rho \\ + \Delta z \int_{R_2}^{R_3} \frac{2\pi J_0}{\rho c} (R_1^2 - R_0^2) - \frac{2\pi J_1}{\rho c} (\rho^2 - R_2^2) d\rho. \end{aligned} \quad (\text{A.7})$$

Integrating results in

$$\begin{aligned} A_z(0) = \left(\frac{2I}{c} \right) \left[\mu \ln \frac{R_2}{R_1} + \frac{1}{2} + \ln \frac{R_3}{R_2} - \frac{R_0^2}{R_1^2 - R_0^2} \ln \frac{R_1}{R_0} \right. \\ \left. + \frac{R_2^2}{R_3^2 - R_2^2} \ln \frac{R_3}{R_2} \right] \end{aligned} \quad (\text{A.8})$$

where we have assumed that the vector potential $A_z(R_3)$ is zero outside the outermost conductor.

In the event that the magnetic permeability μ of the magnetic section is much greater than unity, then the contribution of the magnetic material dominates. In this case, we may write

$$A_z(0) = \frac{2\mu I}{c} \ln \frac{R_2}{R_1}. \quad (\text{A.9})$$

A.3. Looped wire

In the event that a high- μ material is used, then the ratio of vector potential to current can be increased by looping a wire carrying the drive current around the magnetic element, as indicated in figure 2. The vector potential on axis in this case is

$$A_z(0) = \frac{2N\mu I}{c} \ln \frac{R_2}{R_1}, \quad (\text{A.10})$$

where N is the number of windings. The self-inductance of the hollow wire L_{hw} is

$$L_{hw} = \frac{2N^2\mu l_z}{c^2} \ln \frac{R_2}{R_1}, \quad (\text{A.11})$$

where l_z is the length of the hollow wire.

References

- [1] Feynman R 1948 *Phys. Rev.* **74** 1430
- [2] Bethe H A 1947 *Phys. Rev.* **47** 339
- [3] Desiderio A M and Johnson W R 1971 *Phys. Rev. A* **3** 1267
- [4] Mohr P J 1974 *Ann. Phys., NY* **88** 26
- [5] Parle A J 1987 *Aust. J. Phys.* **40** 1
- [6] Eberly J H and Reiss H R 1966 *Phys. Rev.* **145** 1035
- [7] Reiss H R 1979 *Phys. Rev. A* **19** 1140
- [8] Levinson E J and Boal D H 1985 *Phys. Rev. D* **31** 3280
- [9] Barton G 1990 *Ann. Phys. NY* **200** 271
- [10] Donoghue J F, Holstein B R and Robinett R W 1985 *Ann. Phys., NY* **164** 233
- [11] Hollberg L and Hall J L 1984 *Phys. Rev. Lett.* **53** 230
- [12] Reiss H R 1990 *J. Opt. Soc. Am. A* **7** 574
- [13] Widom A and Larsen L 2006 *Eur. Phys. J. C* **46** 107
- [14] Lindroth E and Mårtensson-Pendrill A-M 1989 *Phys. Rev. A* **39** 3794
- [15] Panella O, Widom A and Srivastava Y N 1990 *Phys. Rev. B* **42** 9790
- [16] Pachucki K 2004 *Phys. Rev. A* **69** 052502
- [17] Zawadzki W 2005 *Am. J. Phys.* **73** 756
- [18] Lin D 1977 *Phys. Rev. A* **15** 2324
- [19] Jackson J D 1975 *Classical Electrodynamics* (New York: Wiley)
- [20] Joulin K, Mulet J-P, Marquier F, Carminati R and Greffet J J 2004 *Surf. Sci. Rep.* **57** 59
- [21] Henkel C 2005 *Eur. Phys. J. D* **35** 59
- [22] Henkel C, Joulain K, Carminati R and Greffet J-J 2000 *Opt. Commun.* **186** 57
- [23] Hauer B, Hempelmann R, Udovic T J, Rush J J, Kockelmann W, Schäfer W, Jansen E and Richter D 2004 *J. Phys.: Condens. Matter* **16** 5205
- [24] Knight P L 1971 *J. Phys. A: Gen. Phys.* **5** 417
- [25] Mandel L and Wolf E 1995 *Optical Coherence and Quantum Optics* (New York: Cambridge University Press) (see chapter 18)
- [26] Meltzer D, Davis W and Mandel L 1970 *Appl. Phys. Lett.* **17** 242